

Fabrication of bismuth nanoballs using thermal oil reflow

Chin-Guo KUO, Chien-Chon CHEN,^{*,†} Sheng-Jen HSIEH^{**} and Wen C. SAY^{***}

Department of Industrial Education, National Taiwan Normal University, Taipei, Taiwan, 10610, R.O.C.

^{*}Department of Applied Chemistry, National Chiao Tung University, Hsinchu, Taiwan, 30010, R.O.C.

^{**}Department of Engineering Technology and Department of Mechanical Engineering, Texas A&M University, College Station, TX 77843-3367, USA

^{***}Department of Materials & Mineral Resources Engineering, National Taipei University of Technology, Taipei, Taiwan, 10608, R.O.C.

Sub-micron-size bismuth (Bi) balls with diameters between 100 and 2000 nm were formed on an anodic aluminum oxide (AAO) template using thermal expansion and thermal oil reflow processes. After centrifugal force separation, 100 nm size Bi balls were obtained. In addition, the ball density was approximately $6 \times 10^7/\text{cm}^2$ on an AAO surface. Because of their round shape, the contact angle of the Bi nanoballs on the AAO surface was large after hot oil reflow, making it easy to remove them using ultrasound and to separate different sizes of balls using centrifugal force.

©2008 The Ceramic Society of Japan. All rights reserved.

Key-words : Bi, AAO, Nanoballs, Reflow, Centrifugal force

[Received June 5, 2008; Accepted July 17, 2008]

1. Introduction

Highly regular metal and semiconductor nanorod/nanoball arrays embedded in/on a dielectric matrix have attracted a great deal of research attention because of their potential application in electronic and optical devices. Semimetallic bismuth is a material exhibiting interesting magnetoresistance (MR) characteristics and finite-size effects, and whose electronic properties are fundamentally different from those of common metals due to its complex and highly anisotropic Fermi surface.¹⁾⁻⁷⁾

A promising approach to fabricating nanomaterials is to fill or deposit elements in or on a template. Porous anodic aluminum oxide (AAO), which has hexagonally packed nanometer-sized channels, is one possible host template. Details about the structure and preparation of alumina templates can be found elsewhere.⁸⁾⁻¹⁰⁾ The spacing of the nano-channels can be controlled to some extent by varying process conditions, such as the type, concentration, and temperature of the electrolytic solution used for anodic oxidation, and the amount of voltage applied. For example, varying voltage during the AAO process results in different channel sizes. The relationship between the spacing $2R$ (nm) of the narrow pores and the anodic oxidation voltage V (volts) can be characterized by the empirical relationship $2R = 10 + 2V$. Another Eq., $C = mV$, can be used to characterize the relationship between pore size C (nm) and anodic oxidation voltage V (volts), where m is a constant (2.0–2.5). In this paper, we used AAO as a template to fabricate high aspect ratio Bi nanorods using centrifugal force, and then used thermal expansion and thermal oil reflow processes to fabricate Bi balls. The distribution range of sphere sizes may range from 20 nm to several μm . Stoke's law can be used to evaluate the distribution of particles of various sizes in a suspending liquid. In order to sort small particles with sizes in the sub-micron and nano meter range, centrifugal force can be applied. Our process can quickly produce a large number of Bi balls by using centrifugal force and reflowing processes and then dividing the Bi balls using centrifugal force.

2. Experiment

Bismuth (Bi) nanorods were placed inside an anodic aluminum oxide (AAO) template using centrifugal force. Afterward, the nanorods were expanded in silicate oil to form nanoballs as the oil temperature was raised to the Bi melting temperature. The morphology of the AAO, nanorods, and nanoballs was obtained using atomic force microscopy (AFM) and scanning electron microscopy (SEM). The composition of the nanorods and nanoballs was determined using energy dispersive spectrum analysis (EDS).

Specimens of 99.999% aluminum with dimensions $1\text{cm}^2 \times 0.3$ mm as the substrate were used to prepare AAO. The substrate was annealed at 570°C for two hours and electro-polished at 32 V and $150\text{ mA}/\text{cm}^2$ in a perchloric acid (15%) – ethanol (70%) – monobutylether (15%) bath with stirring at 12°C for 6 min. The specimens were then anodized at 18 V in 10% sulphuric acid electrolyte at 8°C for 3 h, with a platinum plate as the counter electrode. This caused an AAO film with 70 nm pore size and $10\ \mu\text{m}$ thickness to form on the Al substrate, as shown as Fig. 1.

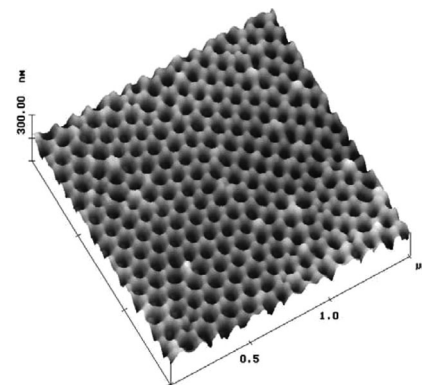


Fig. 1. AFM image of AAO surface; array pores with 70 nm diameter are present on AAO surface after aluminum substrate anodization.

[†] Corresponding author: C.-C. Chen; E-mail: chentexas@gmail.com

Bi nanorods were fabricated using a vacuum centrifugal process. In Fig. 2 is a schematic diagram showing how the AAO and Bi were positioned in the centrifuge. To produce an array of Bi nanorods, the AAO film/Al substrate and Bi piece were placed in a glass tube and sealed using oxygen-acetylene gas to maintain the vacuum (Fig. 2(a)). Then the glass tube was heated up to the Bi melting temperature for 5 min (Fig. 2(b)). In order to prevent the glass tube from breaking in the centrifuge, the hot glass tube was first placed in a titanium tube. A refractory cloth was used to fix the glass in the Ti tube and then the Ti tube cover was closed (Fig. 2(c)) and the tube was placed in the centrifuge. Centrifugal force was applied to push the molten Bi into the AAO template. The centrifuge featured a frequency conversion motor whose maximal rotational speed was 75,000 rotations per minute (rpm), allowing the injection process to be completed in less than a minute. First, the Bi piece was placed on the AAO/Al substrate,

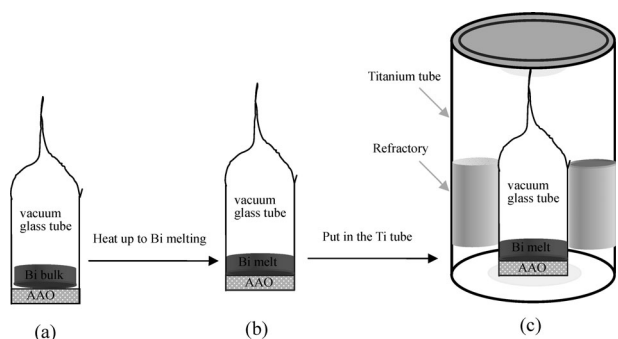


Fig. 2. Schematic diagram of (a) AAO and a piece of Bi put in a vacuum glass, (b) Bi melt cover on the AAO after heating, (c) hot glass tube was put in a titanium tube.

and both were placed in a titanium-tube within which vacuum pressure was maintained at under 10^{-6} torr by using a molecular turbo pump to prevent active Bi oxidation. Then the titanium tube was sealed using oxy-acetylene gas to maintain a vacuum. Before the titanium tube was put on the centrifuge, the tube was heated up to the melting point of Bi (271°C) so that the molten Bi could penetrate the AAO. After centrifugal force was applied, Bi nanorods formed inside the AAO. After the nanorods were formed, the remaining Bi metal was removed from the AAO surface. In order to form Bi nanoballs, the specimen was reflowed in silicate oil. The thermal expansion effect in the hot silicate oil caused the extra molten Bi to come out of the AAO and cover a thin oxide film, forming a ball shape.

To sieve out different sizes of nanospheres, centrifugal force was used. First, a sample of AAO with spheres was placed in an alcohol solution to loosen the spheres from the surface. This

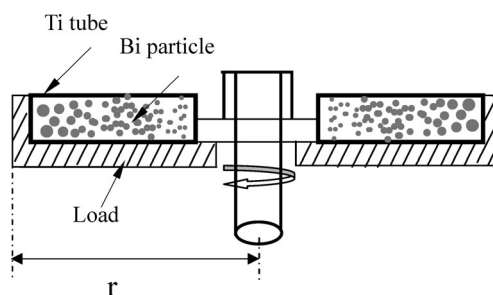


Fig. 3. Schematic diagram of sieve various size of Bi particles by centrifuge.

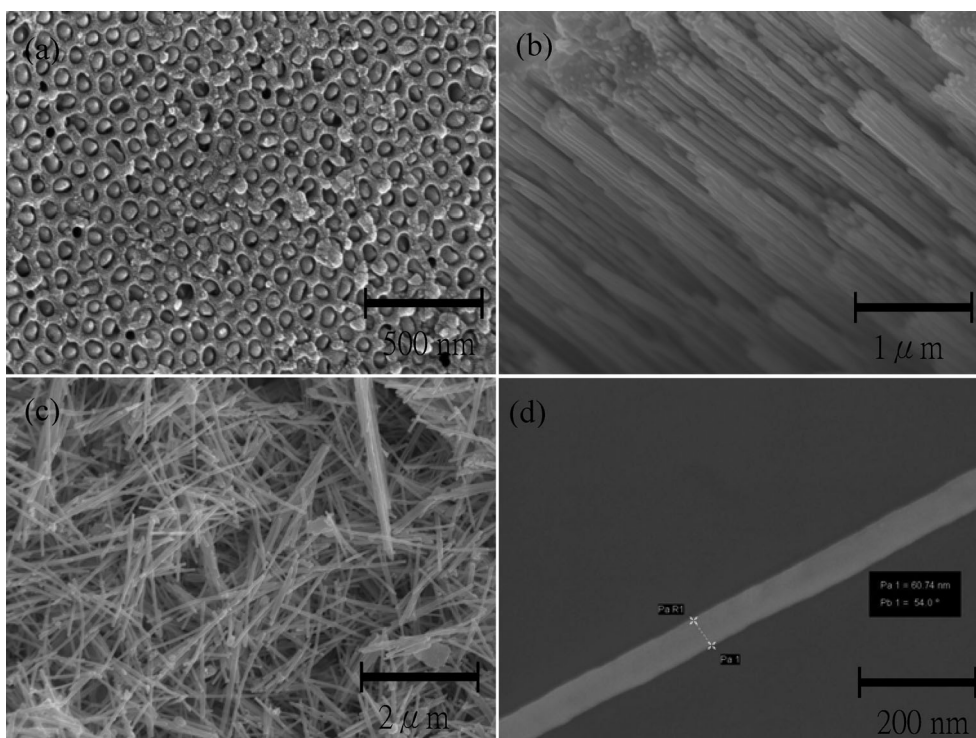


Fig. 4. SEM image of Bi nanorods; (a) top view of Bi melt is injected into AAO channel by centrifugal force and solidifies to form Bi nanorods, (b) side view of Bi nanorods inside AAO, (c) pure Bi nanorods when AAO was dissolved by chemical solution, (d) single Bi nanorods.

allows sub-micron and nano scale spheres to be removed from the AAO surface using ultrasound. Centrifugal force was then applied to the solution so that spheres of different sizes could be separated out, as shown in the schematic diagram in **Fig. 3**.

3. Results and discussion

Bismuth has a low melting point (271°C) and is an active metal. It easily reacts with oxygen in the surrounding air to form oxides of Bi_2O_3 when melted. Therefore, the bismuth melt must be kept in a vacuum chamber when the Bi is injected into AAO channels using centrifugal force. In our experiment, the Bi melt was kept in a Ti vacuum tube. Because Ti is more active than Bi, the remaining oxygen in the tube reacts with Ti first to avoid Bi oxidation. For example, the equilibrium partial oxygen pressure of Ti– TiO_2 and Bi– Bi_2O_3 are $10^{-80.41}$ atm and $10^{-27.09}$ atm respectively at 275°C,¹¹⁾ which means that Ti is oxidized more easily than Bi. The pore size and thickness of the AAO we used were 70 nm and 10 μm , respectively. When the rotational speed of the centrifuge reached 8,000 rpm (4,216 G), the Bi melt could be injected into the AAO to form Bi nanorods. **Figure 4** shows the SEM images of nanorods. (a) Top view image of the high filling ratio of Bi in AAO, and (b) the side view image of Bi nanorods inside the AAO and the rod size was depended on the AAO pore diameter and tube length. Moreover, to collect free-standing Bi nanowires, the AAO template was dissolved thoroughly in 0.2 wt.% sodium hydroxide (NaOH) solution at $\sim 23^\circ\text{C}$ for 2 h. (c) The image showed pure Bi nanorods when AAO was dissolved by chemical solution. (d) In order to collect single Bi nanorods the nanorods were then transferred into 0.5 ml isopropanol and dispersed by sonication. A drop of the isopropanol suspension was dropped onto Cu grid with carbon film for single nanorods observation.

In order to obtain Bi balls on the AAO, the specimen (nano-

rods inside AAO) was removed from the titanium tube and placed in hot silicate oil (275°C) with a temperature a little higher than the melting point of Bi (271°C). After 5 s of immersion time, the specimen was removed from the hot silicate oil and exposed to air. Because of linear thermal expansion of the nanorods, part of Bi melt can be extruded and formed on the AAO, as shown as **Fig. 5**. The metal linear thermal expansion can be estimated by $l_t = l_0(1 + \alpha \times t)$, where l_0 is the length at 273K (0□), α is the coefficient of linear thermal expansion (Bi = $13.6 \times 10^{-6}/\text{K}$),¹²⁾ and l_t is the length at temperature t . Because Bi has high surface tension (378 dyne/cm),¹³⁾ the extra Bi on the AAO surface easily forms balls when the melt is solidified and reflowed in oil. As predicted by a linear thermal expansion Eq., Bi ball sizes increase as temperature increases. In order to obtain

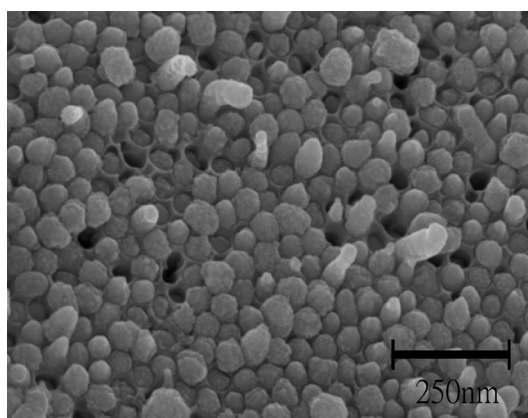


Fig. 5. Bi metal expands and comes out on the AAO surface when temperature is at 275°C for 5 s.

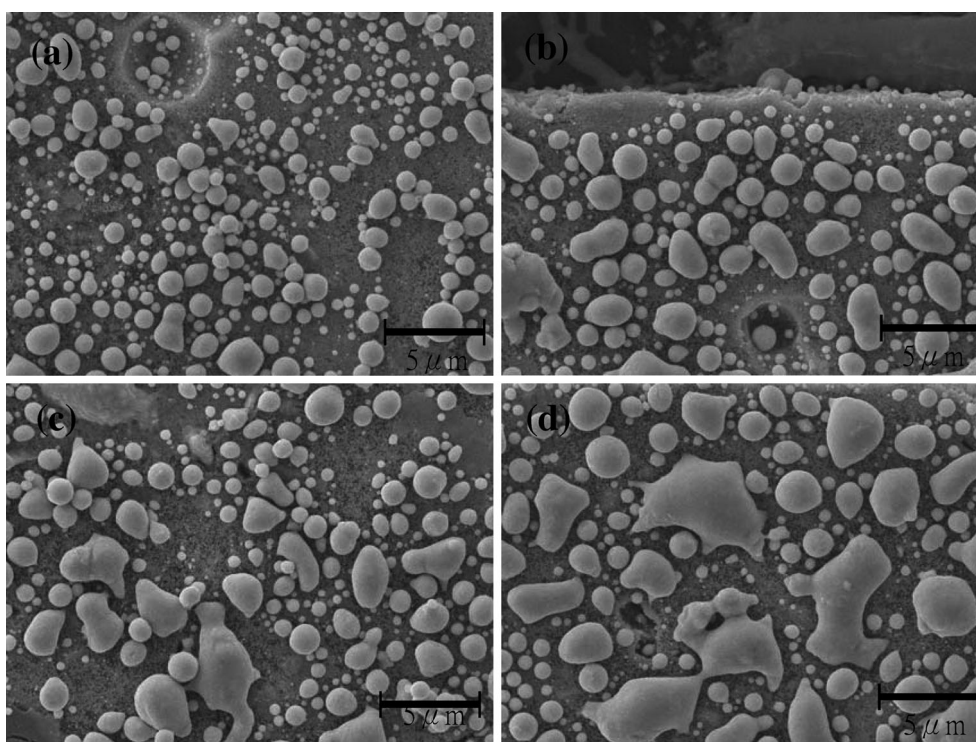


Fig. 6. Thermal expansion due to long heating duration causes Bi melt merging on AAO surface at 275°C; (a) 1 min, (b) 3 min, (c) 5 min, (d) 8 min.

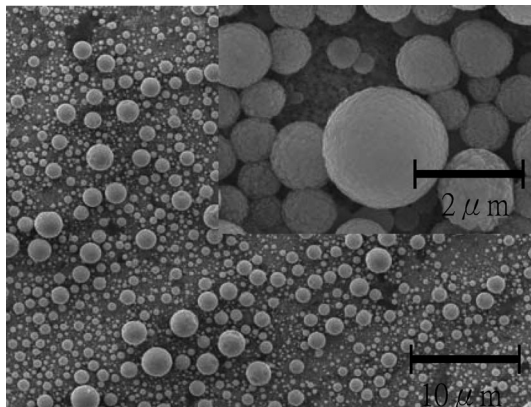


Fig. 7. A suitable heating time of 25 s at 275°C caused Bi to thermally expand and form balls.

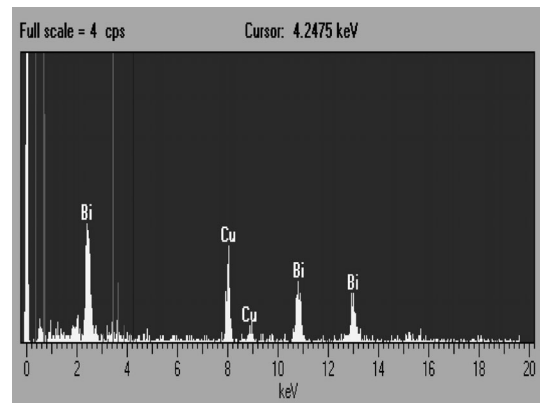


Fig. 8. EDS peaks showed the composition of balls is pure Bi.

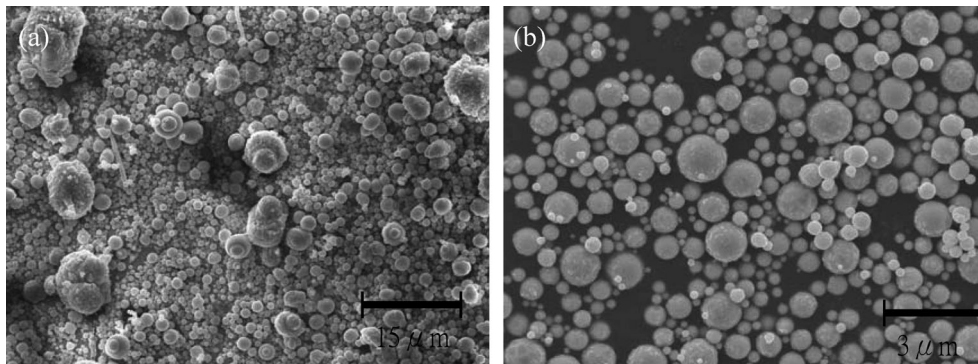


Fig. 9. SEM pictures showed (a) various sizes of Bi particles agglomerate together when ultrasound is used to remove particles from the AAO surface, (b) Bi particle sizes from 0.3 μm to 3 μm can be collected through a 30-min centrifugal process.

small Bi ball sizes, the temperature must be kept a little higher than the Bi melting point (we used 275°C in our experiments). However, the emerging balls merge easily when heating time increases. **Figure 6** shows how the Bi balls merge together when subjected to various heating durations at 275°C. Figure 6(a) shows that the drops merged together and ball size was between 200 nm to 2 μm when the heating time was 1 min. Figure 6(b) shows ball sizes between 300 nm to 2 μm when the heating time was 3 min. When a number of balls merge together, the ball shape will no longer appear because the effects of gravity exceed the surface tension of the ball; in addition, the shape of the ball will tend to merge. For example, with longer heating durations as shown in Fig. 6(c) (5 min) and Fig. 6(d) (8 min), the merging can be observed using SEM images. In order to form balls and prevent balls from merging together, the critical heating time for ball formation needs to be controlled. The critical heating time is that time between when the extra Bi melt comes out (Fig. 5) and when the balls merge (Fig. 6(a)).

In our experiment results, when the heating duration was 25 sec at 275°C, the extra Bi melt could form balls with diameters between 100 nm and 3 μm, as shown in **Fig. 7**. In addition, the Bi balls were then corrected on the copper grid. **Figure 8** shows the EDS peaks presenting the composition of the balls are pure Bi, and Cu peaks are relate to copper grid. Our process makes it easy to fabricate Bi balls on an AAO surface; however, it is difficult to obtain a uniform ball size when collecting balls using ultrasound. For example, **Fig. 9(a)** shows that balls agglomerate

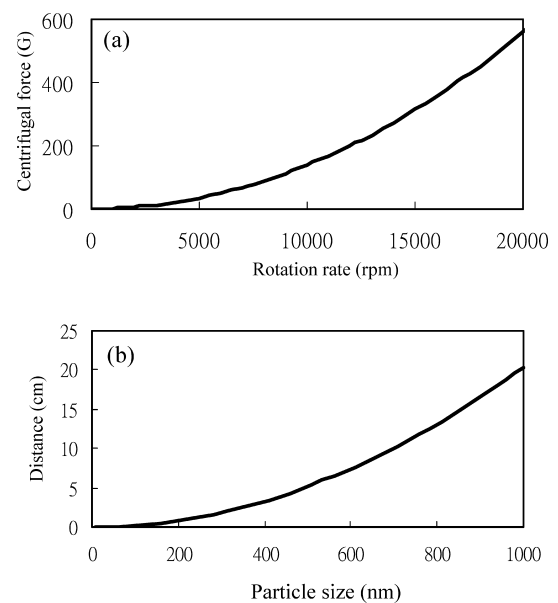


Fig. 10. Curves showed (a) centrifugal acceleration with rotation rate and (b) particle size distribution in alcohol with distance from centrifugal center at 300 G for 4 min.

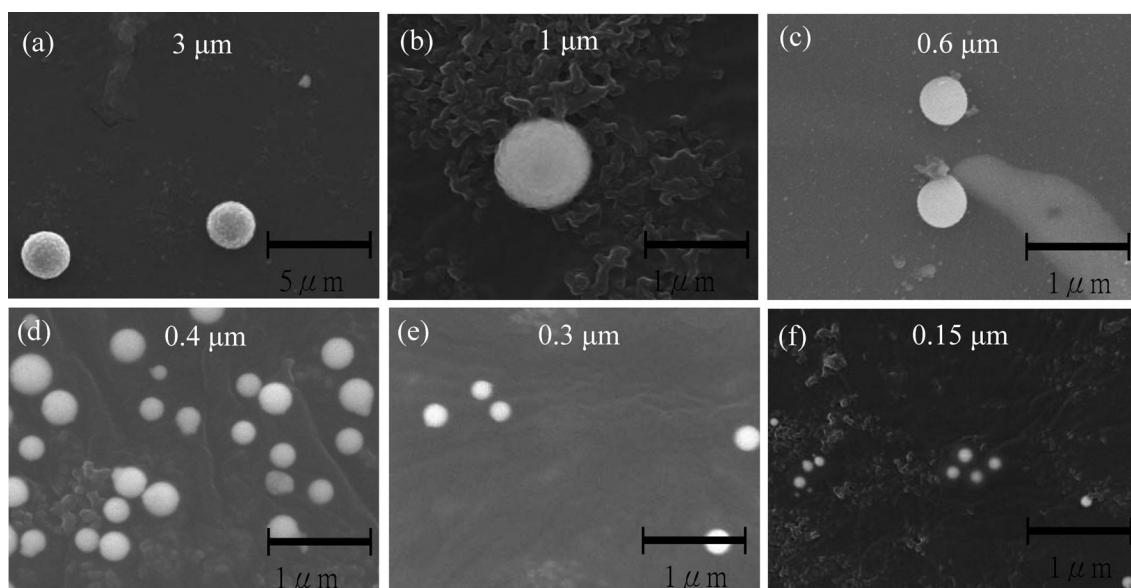


Fig. 11. Bi balls with 3 μm to 0.15 μm size were collected from the centrifugal tube. (a) 3 μm Bi ball was collected from the tube bottom, (b) 1 μm Bi ball was collected from the 22 cm position of centrifugal radius, (c) 0.6 μm from 8 cm position, (d) 0.4 μm from 4 cm position, (e) 0.3 μm from 2 cm position, and (f) 0.15 μm from 0.5 cm position.

easily when collected from AAO using ultrasound in liquid oil. To remedy the agglomeration problem, a centrifuge can be used to provide a large centrifugal force to nanoparticles. Figure 9(b) shows that when the balls in Fig. 9(a) have been sieved in a centrifuge at 90 G (G is gravitational constant) or 8000 rpm for 3 min, most of the large agglomerations can be distributed into small particles. However, the particle sizes in Fig. 9(b) are in the 0.3 μm to 3 μm range. Larger centrifugal force or longer centrifugal time is needed for 0.3 μm to 3 μm size particles to be distributed. In Fig. 9, the centrifugal system offers 90 G (8000 rpm) to the teat sample which is Bi nanoballs (0.3 μm to 3 μm) solution. According to 8000 rpm of angular speed, the centrifugal force on 0.3 μm to 3 μm Bi nanoballs (0.008 to 225×10^{-12} G) can be calculated as $F = 4\pi r^3 \rho R \omega^2 / 3$, where F is centrifugal force, r is Bi ball radius, ρ is Bi density (9780 kg m^{-3}), R is radius of centrifugation, and ω is the angular speed.

Centrifugal force is a physical force that increases with rotation rate, centrifugal radius, and the mass of the sample on the centrifuge. Centrifugal force¹⁴⁾ is given by $F = mR\omega^2$ where F is centrifugal force (N); m is the mass of the sample (kg); R is the radius of centrifugation (m), and ω is the angular speed (rad/s). In this experiment, the mass of the sample was 50 g, and the radius of centrifugation was 25 cm. Therefore, the centrifugal force (G) with rotation rate (rpm) curve can be drawn as shown in Fig. 10(a). A centrifuge is useful for dividing nanoparticles in a narrow distribution of particle sizes. In the settling process, larger particles settle faster than small ones, based on Stoke's law,¹⁵⁾

$$t_x = \frac{18\eta h}{(\rho - \rho_F)gx^2}, \text{ where } t_x \text{ is the time for a particle of size } x \text{ to}$$

settle through the distance h from the top of the suspension to the bottom, η is the viscosity of the liquid, ρ and ρ_F are the densities of the particles and the suspending liquid respectively, and the g is the gravitational constant. Since nanoparticles have smaller volume and less mass in comparison to micron particles, it is difficult to divide them into various sizes using a normal settling process. However, when centrifugal force is increased

as specified in Stoke's law, nanoparticles of various mass can be separated easily. In our experiment, the density ρ of Bi is $9870 \text{ (kg/m}^3\text{)}$, the density ρ_F of alcohol is $780 \text{ (kg/m}^3\text{)}$, and the viscosity of alcohol is $0.00175 \text{ (pa}\cdot\text{s)}$ at 2°C . When centrifugal force is 300 G (14700 rpm) for 4 minutes, the curve of sphere sizes with relative distance of centrifugal center can be estimated as in Fig. 10(b). According to calculations based on Fig. 10, we placed our sample in alcohol, set it in the centrifuge, applied 300 G for 4 minutes, and then collected Bi particles using a dropper. In Fig. 11 shows that Bi balls of various sizes ranging from 0.15 μm to 3 μm were collected from the centrifugal tube and that the Bi ball positions were between 0.5 cm and 25 cm on the centrifugal radius.

4. Conclusions

We have successfully fabricated high aspect ratio Bi nanorods using centrifugal force. Additionally, Bi nanorods can be extruded from AAO channels to form Bi balls on the surface due to thermal expansion and oil reflow effects, which accomplishes the fabrication of Bi nanorods/balls with cost-effectiveness and simplicity in operation. Different graded sizes of Bi nanospheres were sieved out and collected using a centrifugal force-based settling process. The uniform pore size and roughness of AAO offers a suitable position for Bi ball formation. Our process has the potential to yield metal balls with sizes smaller than 100 nm when pore diameter and AAO thickness are reduced.

References

- 1) K. Liu, C. L. Chien and P. C. Searson, *Phys. Rev. B*, **58**, R14681–R14684 (1998).
- 2) M. Lu, R. J. Zieve, A. van Hulst, H. M. Jaeger, T. F. Rosenbaum and S. Radelaar, *Phys. Rev. B*, **53**, 1609–1615 (1996).
- 3) J. H. Mangez, J. P. Issi and J. Heremans, *Phys. Rev. B*, **14**, 4381–4385 (1976).
- 4) Stuart Golin, *Phys. Rev.*, **166**, 643–651 (1968).
- 5) N. Garcia and Y. H. Kao, *Phys. Rev. B*, **5**, 2029–2039 (1972).

- 6) R. D. Brown, R. L. Hartman and S. H. Koenig, *Phys. Rev.*, **172**, 598–602 (1968).
- 7) F. Y. Yang, K. Liu, K. Hong, D. H. Reich, P. C. Searson and C. L. Chien, *Science*, **284**, 1335–1337 (1999).
- 8) G. E. Thompson and G. C. Wood, *Nature*, **290**, 230–232 (1981).
- 9) J. Li, C. Papadopoulos and J. Xu, Nanoelectronics, *Nature*, **253**, 253–254 (1999).
- 10) H. Masuda and K. Fukuda, *Science*, **268**, 1466–1468 (1995).
- 11) Syverud, JANAF Thermochemical Table, 3rd ed., *J. Phys. Chem. Ref. Data* (1985).
- 12) D. R. Lide, Chemical Rubber Company Handbook of Chemistry and Physics, Florida, USA, 79th edition (1998).
- 13) Z. Zhang, X. Sun, M. S. Dresselhaus and J. Y. Ying, *Appl. Phys. Letts.*, **73**, 1589–1591 (1998).
- 14) V. E. Vergara and N. V. Salazar, *J. Mater. Proces. Tech.*, **63**, 765 (1997).
- 15) F. V. Lenel, “Powder Metallurgy: Principles and Applications,” Metal Powder Industries Federation, New Jersey, USA (1980) p. 63.